Nexus Netw J (2014) 16:251–271
DOI 10.1007/s00004-014-0187-7

NEXUS NETWORK JOURNAL
Architecture and Mathematics

RESEARCH

The Fractal Pattern of the French Gothic Cathedrals

Albert Samper · Blas Herrera

Published online: 9 May 2014

Abstract The classic patterns of Euclidean Geometry were used in the construction of the Gothic cathedrals to provide them with proportion and beauty. Still, there is also another complex concept related to them: the un-evenness of their structures, which determines their space-filling ability, that is, their level of roughness. In this paper we use the techniques of Fractal Geometry to generate parameters which provide a measure of roughness. In this way we show that the French Gothic cathedrals do not only follow Euclidean geometric patterns, but also have a general non-random fractal pattern.

Keywords French Gothic · Fractal parameter · Fractal dimension · Gothic architecture

Introduction

Benoit Mandelbrot was the main developer of Fractal Geometry in the late 1970s. His theories have evolved and have been used in several fields including architecture. Inspired by Mandelbrot's work, Bechhoefer and Bovill used the concept of fractal dimension in architectural drawings (Bechhoefer and Bovill 1994; Bovill 1996). As a result of this work, many authors (see Ostwald et al. 2008; Vaughan and Ostwald 2009, 2010, 2011; Ostwald and Vaughan 2009, 2010) used similar techniques to analyze the design of certain architects such as Le Corbusier,

A. Samper
Unitat predepartamental d'Arquitectura, Universitat Rovira i Virgili,
Avinguda Països Catalans 26, 43007 Tarragona, Spain

B. Herrera (✉)
Departament d'Enginyeria Informàtica i Matemàtiques, Universitat Rovira i Virgili,
Avinguda Països Catalans 26, 43007 Tarragona, Spain
e-mail: blas.herrera@urv.net

Frank Lloyd Wright, Peter Eisenman and Eileen Gray. Specifically, those authors looked for a relation between the structure of the architects' constructions and the natural or artificial environment where those constructions were projected. These techniques have also been used in other kinds of architectural studies (see Bovill 1996; Eglash 1999; Batty and Longley 2001; Burkle-Elizondo 2001; Ostwald 2001, 2010; Crompton 2002; Brown and Witschey 2003; Cooper 2003; Sala 2006; Hammer 2006; Joye 2007; Rian et al. 2007; Bovill 2008; Ostwald and Vaughan 2013). These works are based on a geometrical concept which is called *fractal dimension*. In this paper we will use this concept in order to generate what we will call *fractal parameter*; and by means of this parameter we will study the existence of a yet unknown pattern in French Gothic cathedrals. This generated fractal parameter will give a measure of the unevenness of their structures, which in turn determines their space-filling ability, which is also a measure of their level of roughness.

Historical Setting

Gothic cathedrals are widely accepted as being among the most important art creations of mankind. They are the result of religious interests, aesthetic patterns and social influences, and their making brought together great scientific know-how (Wilson 1990; Baldellou 1995; Toman 1998; Prache 2000; Schütz 2008). The style of architecture we now call Gothic first emerged between the 12th and 15th centuries of the medieval period. It emphasized structural lightness and illumination of the inside naves. It arises in contrast to the massiveness and the inadequate interior illumination of Romanic churches. It evolved mainly within ecclesiastical architecture, especially cathedrals.

Gothic art was born in northern France, in a region called "Île de France" to be precise. Historically, this style was marked by the alliance between the French monarchy and the Catholic Church. The first trial of Gothic architecture took place in Saint Denis under the patronage of abbot Suger, friend and confident of Louis VI. Following the example of Saint Denis, several primeval Gothic buildings were built in the second half of the 12th century. In Laon cathedral (1156–1160) and Notre Dame cathedral (1163), the central nave was raised and the light became the dominant element. It was also then that construction of Chartres cathedral began. There, the architect abandoned entirely the use of the tribune gallery and introduced the use of simple ribbed vaults. From the 13th century onward, after these first trials, the Gothic style entered its classical stage. The best examples are the Reims cathedral (1211) and the Amiens cathedral (1220). Both have a cross-shaped floor plan and their elements were combined in pursuit of illumination and structural lightness and regularity. The classical Gothic style was adapted in France into numerous regional ramifications.

Significant Sample and Geometrical Patterns

Our study focuses into a subset of 20 French cathedrals which are predominantly Gothic in style, were built in the region called Île de France between the 11th and

13th centuries, and are representative of the total population of Gothic cathedrals (Fig. 1).

This sample of cathedrals is considered to be significant in stylistic, chronological and geographical terms. We intend to analyse the constructions geometrically using new parameters which were unknown until now. Since each construction had its very own authorship and circumstances, we have not gone on to compare cathedrals with each other. Instead, we have examined if the design traits and structures of these constructions have a deeper geometrical sense than is known to us yet.

Fig. 1 Geographical situation of the 20 cathedrals being studied: Strasbourg cathedral (1015), Troyes cathedral (1128), Sens cathedral (1135), Noyon cathedral (1150), Senlis cathedral (1153), Laon cathedral (1155), Paris cathedral (1163), Lisieux cathedral (1170), Tours cathedral (1170), Soissons cathedral (1177), Chartres cathedral (1195), Bourges cathedral (1195), Rouen cathedral (1202), Reims cathedral (1211), Auxerre cathedral (1215), Amiens cathedral (1220), Metz cathedral (1220), Orleans cathedral (1278), Toul cathedral (13th century), Sées cathedral (13th–14th century)

The master craftsman had to be extensively knowledgeable about mathematics, particularly about geometry, as we can see from the sketchbooks of architect Villard de Honnecourt (Bechmann 1985). We must bear in mind that they didn't have a precise scale to measure fractions smaller than a toise or a foot-length and transport them accurately to bigger units. Therefore, it was safer to take a geometric outline as the starting point for the construction; for instance a square mesh like the ones used for the Roman and pre-Gothic basilicas and for the Roman fortified camps. As well as the square, architects used the pentagon, the octagon and the decagon (all of them constructible using a ruler and a compass) to represent, by means of accurate geometric relations, the floor plans and elevations of their constructions (Simon 1985). The square, as well as the octagon, stemmed from geometries which took the heavenly Jerusalem as a model. Nonetheless, the most perfect proportion stems from the pentagon and the decagon, leading to the golden ratio phi (Fig. 2).

The classic patterns of the Euclidean Geometry, such as coefficients phi and pi, were used in Gothic constructions to provide them with proportion and beauty (Fig. 3). As well as the Euclidean elements, however, there is another complex concept in the construction of the Gothic cathedrals: the unevenness of their structures, which determines their space-filling ability, i.e. their level of roughness. The best tool to describe this concept is given by Fractal Geometry through a ratio called *fractal dimension*. We will generate a geometrical parameter, called *fractal*

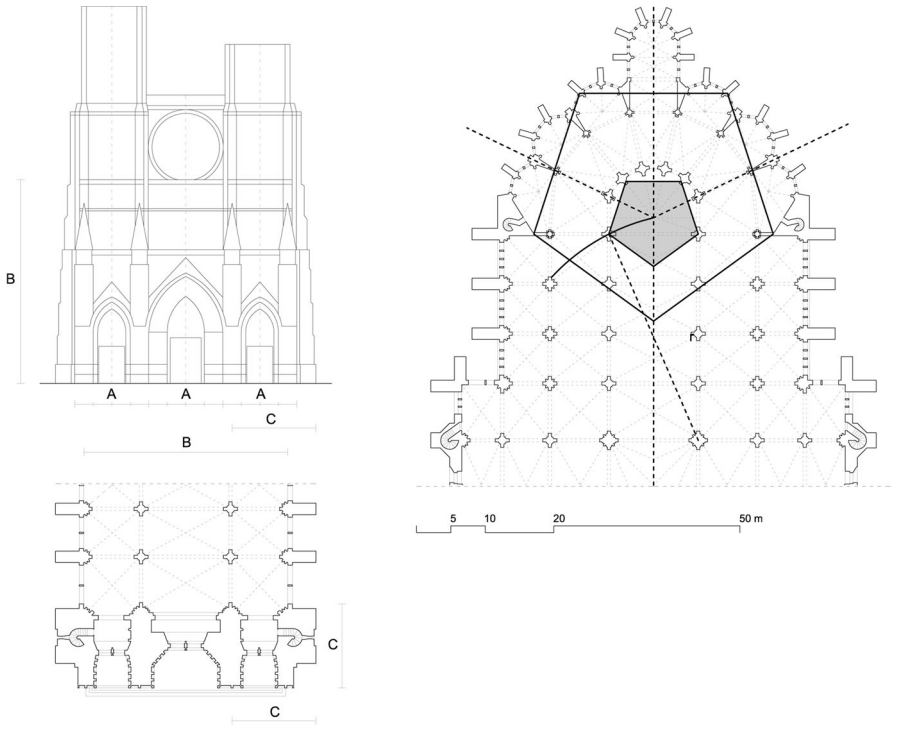

Fig. 2 Amiens Cathedral, geometric development of the Floor plan

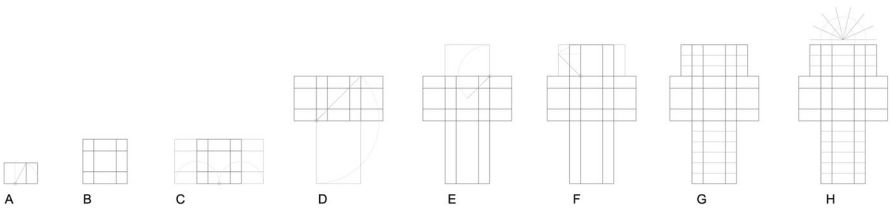

Fig. 3 Amiens Cathedral, geometric outline. Module A is 40 feet; module B is 110 feet

parameter, which will give a measure of roughness. As well as being attributable to Euclidean elements, this fractal parameter is generated by the final architectonic result of the constructions.

The aim of our investigation is to analyse the geometry of the French Gothic cathedrals in order to show the existence of a general fractal pattern. We are not comparing the constructive processes of the cathedrals nor the will of the architects to implement their designs. Instead, we will demonstrate that the geometry of their compositions shows a common formal pattern.

Fractal Parameter and Method

The first step of our investigation was to collect as many graphic documents as possible from all the cathedrals being studied. The main information sources were: the respective archdioceses of the cathedrals (we thank them for providing us with specially clear and precise graphic papers); Jean-Charles Forgeret, in charge of the Médiathèque de l'Architecture et du Patrimoine, who provided us with original historical drawings for the different parts of each cathedral; Martine Mauvieux, in charge of the Département des Estampes et de la Photographie de la Bibliothèque Nationale de France, who offered a large number of photographs and drawings which we used for redrawing; the Archivo del Colegio de Arquitectos de Catalunya; and the Biblioteca de la Escuela Técnica Superior de Arquitectura de Barcelona, where we found some very illustrative monographs (see Murray 1996; Kunst and Schekluhn 1996) which let us complete the study.

All documents collected have been redrawn by us with CAD tools in order to attain the highest level of objectivity, homogeneous graphic display criteria and the same level of detail, without taking textures into account (Ostwald and Vaughan 2013), using black color and line width $\sim$0.00 mm (that is, the minimal lineweight allowed using CAD software), see Fig. 4. This was absolutely necessary, since the information collected had different styles and, in general, a very low, inadequate resolution to be able to apply the calculations.

So, in order to establish the fractal parameter of the French Gothic architecture, we leave ornaments aside and we take three basic projections of the cathedral's structure: floor plan, main elevation and cross-section. Working on these projections, we make the corresponding mathematical calculations. Figure 4 shows the detail level of the redrawing. Figures 7, 8 and 9 show the redrawing made for

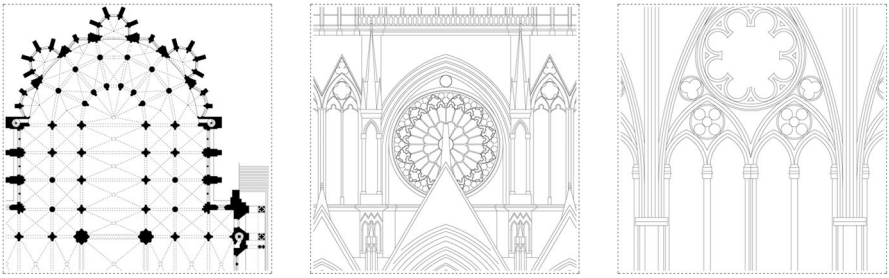

Fig. 4 Detail level of the redrawings: on the *left*, a detail of Chartres cathedral's ambulatory. In the *middle*, a detail of Reims cathedral's main elevation. On the *right*, a detail of a module of the central nave's cross-section in Amiens Cathedral

these basic projections of the 20 cathedrals being studied (redrawing is in a small scale to keep the paper reasonably short).

We have strictly followed precise drawing lines, highlighting the lines which best represent the geometry of the floor plan, main elevation and cross-section. As we have stated before, this redrawing is absolutely necessary, since the documents collected consist of drawings or photographs with shadows, stains, colors, defects, freehand lines, etc.; i.e. all graphic documents show "noise", so we had to do again each and every one of the drawings which appear in this paper.

Summary of the Fractal Parameter's Generation Process

Architectural structures, from now on called M, are not fractal objects. Despite that, we can consider M's unevenness and its space-filling ability, that is, its level of roughness. Also, we can generate a parameter for these non-fractal objects, the *fractal parameter* $P_s(M)$. The value provided by this fractal parameter $P_s(M)$ is a measure of the level of roughness of the architectural structure being studied M.

The process to generate $P_s(M)$ through calculations with a self-created software is summarized as follows:

1. Given the architectural structure M, first we generate its design in AutoCad vector format, using black color and line width $\sim$0.00 mm. From this AutoCad format we obtain the pdf vector format.
2. From the pdf vector format we generate a black-and-white digital bitmap file, sized 1,024 $\times$ υ pixels, showing the architectural structure with its size adjusted to full width and height.
3. $P_s(M)$—using a self-created software, we calculate the fractal parameter $P_s(M)$ based on the slope on the last point of a continuous graph ln–ln. In the following sections we explain which continuous graph we are talking about and which calculations are made.

The value $P_s(M)$ is a fractal parameter of the structure M, which gives a measure of its level of roughness.

The reason to create for ourselves a special software is twofold: firstly, we will have total control of the calculations and so we will ensure these calculations are correct. Secondly, commercial software like Benoit does not use the slope on the last point of the continuous graph ln–ln. Benoit uses the slope of the regression line corresponding to the discrete set of points in the graph ln–ln.

However, the slope of the regression line is only similar to the fractal dimension when M is a fractal self-similar object, because then its continuous graph ln–ln is a straight line. But an architectural structure M is not a fractal object nor a self-similar fractal object, so its continuous graph ln–ln is not a straight line (later on we will define a fractal object and a fractal self-similar object). M does not possess fractal geometry but it does have a fractal parameter $P_s(M)$; we will generate this parameter $P_s(M)$ with a process which has been extrapolated from the theoretical limit $\bar{F}(M)$, called upper fractal dimension of M, M being a non self-similar fractal object (this process will be explained later).

In any case, if we change step 3 above and instead we use the calculation for the slope of the regression line corresponding to the discrete set of points, then we obtain another fractal parameter which we will call $P_r(M)$. For this calculation we can use either our self-created software or Benoit. Then step 3 is as follows:

3. $P_r(M)$—using either a self-created software or the commercial software Benoit, we calculate the fractal parameter $P_r(M)$ based on the slope of the regression line corresponding to the discrete set of points in the graph ln–ln; and for this calculation we use square meshes, the finest mesh having 4×4 pixel squares, and the coarsest mesh having 32×32 pixel squares.

The reason for using square meshes with these particular limits of fineness and coarseness will be explained later.

We may also consider another variation of the fractal parameter if we change step 3 of the process above and instead we make the calculations with the variables which the commercial software Benoit uses by default. The new parameter thus obtained is called $P_b(M)$. Then step 3 is as follows:

3. $P_b(M)$—using the commercial software Benoit we calculate the fractal parameter $P_b(M)$ based on the regression line corresponding to the discrete set of points in the graph ln–ln, and for this calculation we use square meshes, the finest mesh having 1×1 pixel squares and the coarsest mesh having 256×256 pixel squares.

To sum up, we have created software to obtain the value $P_s(M)$ because the structures M being considered are not self-similar objects, but we also calculate the values $P_r(M)$ and $P_b(M)$. These three measures are not equal because the calculation methods are different. However, all three give a measure of the roughness of the structure.

In this paper we calculate and use the three parameters $P_s(M)$, $P_r(M)$ and $P_b(M)$ in order to show, beyond any doubt, the existence of a fractal pattern in Gothic structures. At the end of this paper we will see the results and relationships between the three measures.

Hausdorff–Besicovitch Dimension

Readers may skip this very technical subsection and still fully understand the work which is presented in this paper. We provide book references to interest readers. In this section we summarize the dimensions $T(M), \mathcal{H}(M), \bar{F}(M), F(M), H(M), S(M)$ of the fractal objects M; and some of their properties. This is the theoretical basis from which the ideas for generating the fractal parameter $P_s(M)$ arise.

Let M be a bounded non-empty subset of the n-dimensional Euclidean affine space, $\mathbb{A}^n$. The definition of the *s-dimensional Hausdorff measure of M*, $\mathcal{H}^s(M)$, can be found in (Falconer 1990, 1997; Edgar 1998) or in other books about fractals. There is also a theorem which states as follows: there is a critical value $\mathcal{H}(M)$ such that: $\mathcal{H}^s(M) = \infty$ if $0 \leq s < \mathcal{H}(M)$, and $\mathcal{H}^s(M) = 0$ if $s > \mathcal{H}(M)$. If $s = \mathcal{H}(M)$, then $\mathcal{H}^s(M) \in [0, \infty]$. This critical value $\mathcal{H}(M)$ is called *Hausdoff-Besicovitch dimension of M*. Moreover, M has its *topological dimension*, *T (M)*. We have the following geometric definition: M is a *fractal object* if $\mathcal{H}(M) > T\ (M)$.

The Hausdorff–Besicovitch dimension has an upper bound $\bar{F}(M) > H(M)$. This upper bound $\bar{F}(M)$ is called *Minkowski-Bouligand dimension of* $M \subset \mathbb{A}^n$, and we will call it *upper fractal dimension of M*. The object M can be fractal or not, but in any case the upper fractal dimension $\bar{F}(M)$ is a measure of the level of roughness of M; i.e. it is a measure of the unevenness of the structures, which determines their space-filling ability.

In the above-mentioned books, the reader can see that the definition of $\bar{F}(M)$ is as follows: let $N_e(M)$ be the smallest number of sets of diameter at most $\varepsilon > 0$ which can cover M. The upper fractal dimension of M is defined as $\bar{F}(M) = \limsup_{\varepsilon \to 0} \frac{In(N_e(M))}{-In(\varepsilon)}$

Also in those books, we can find the theorem which states that:

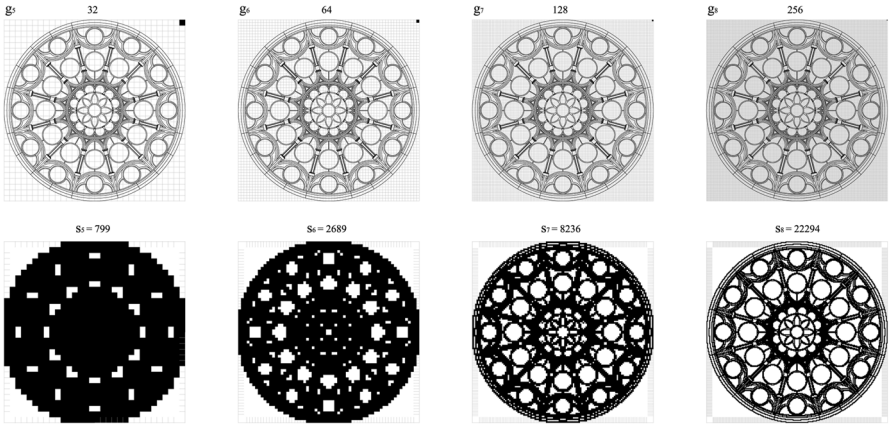

Fig. 5 *Square* meshes g_5, g_6, g_7, g_8 and vectors $(h_5, h_6, h_7, h_8) = (32,\ 64,\ 128,\ 256)$, $(s_5, s_6, s_7, s_8) = (799,\ 2689,\ 8236,\ 22294)$ in the calculation of the fractal parameter P_s for the rose window in the transept elevation of Reims cathedral

$$\bar{F}(M) = \limsup_{m\to\infty} \frac{In(N_m(M))}{-In(2^m)}$$

where $1/2^m = \delta$ and $N_m(M)$ is the number of δ-mesh cubes of $\mathbb{A}^n$ that intersect M. For this reason $\bar{F}(M)$ is also called *upper box-counting fractal dimension.*

If $\bar{F}(M) = \limsup_{\varepsilon\to 0} \frac{In(N_\varepsilon(M))}{-In(1/\varepsilon)}$ is equal to $\liminf_{\varepsilon\to 0} \frac{In(N_\varepsilon(M))}{In(1/\varepsilon)}$, then the limit $\lim_{\varepsilon\to 0} \frac{In(N_\varepsilon(M))}{In(1/\varepsilon)} = F(M)$ exists and $\bar{F}(M) = F(M)$. This limit $F(M)$, if it exists, is called the *fractal dimension* of *M, (box counting fractal dimension of M).*

Let (M, N) be a pair of bounded non-empty subsets of $\mathbb{A}^n$, such that: $M = h_r(N)$, where h_r is a homothety of ratio r, and $M = \coprod_{i=1}^{i-m} g_i(N)$, a disjoint union, where g_i is a displacement. Then M is called a *homothetic object*, and its *homothetic dimension* is $H(M) = \log_r(n)$, i.e. $r^{H(M)} = n$. If M is a homothetic object and $H(M) \neq T(M)$, then M is a fractal object. A homothetic object is a particular case of the following objects called self-similar objects.

Let M be a bounded non-empty subset of $\mathbb{A}^n$, such that: $M = \coprod_{i=1}^{i-m} S_i(N)$ where S_i is a contractive similarity; i.e. $S_i : \mathbb{A}^n \to \mathbb{A}^n$ such that $\forall(x, y) \in \mathbb{A}^n \times \mathbb{A}^n \Rightarrow d(S_i(x), S_i(y)) = k_i d(x, y)$ with $0 < k_i < 1$. Then M is called a *self-similar object*, and its *self-similarity dimension* is the value $S(M)$ such that $\sum_{i=1}^{i=m} k_i^{S(M)} = 1$. If M is

Table 1 Data corresponding to Fig. 5

g_n	a_n	h_n	s_n	ln (2^n)	ln(s_n)
g_5	32	32	799	ln (2^5)	ln(799)
g_6	16	64	2,689	ln (2^6)	ln(2689)
g_7	8	128	8,236	ln (2^7)	ln(8236)
g_8	4	256	22,294	ln (2^8)	ln(22294)

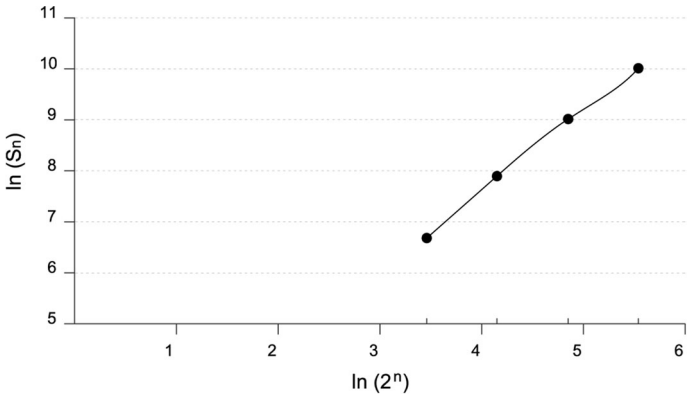

Fig. 6 Continuous graph ln–ln resulting from Table 1, taking the example of the rose window in the transept elevation of Reims cathedral

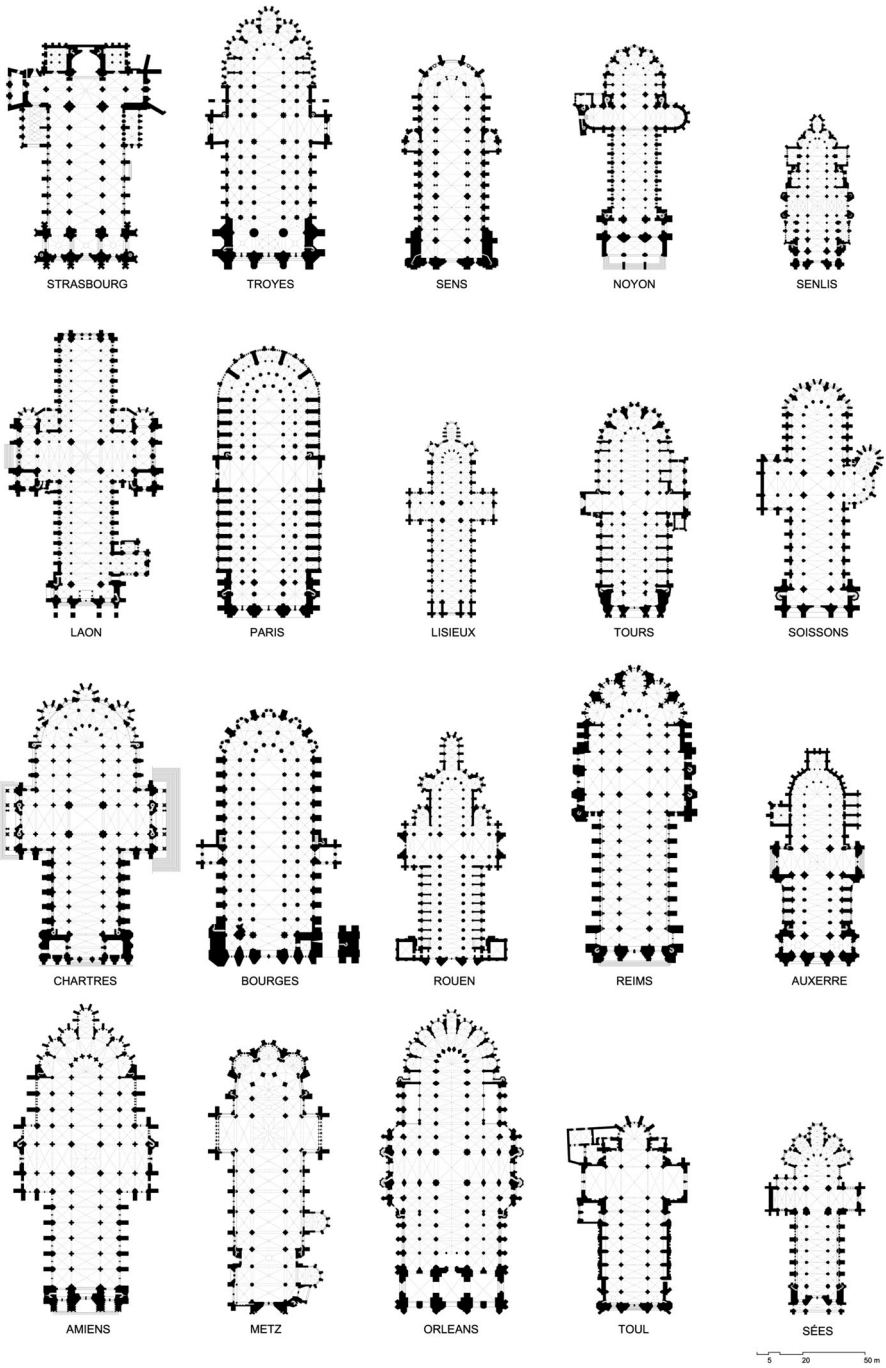

Fig. 7 Floor plans of the cathedrals being studied, in chronological order

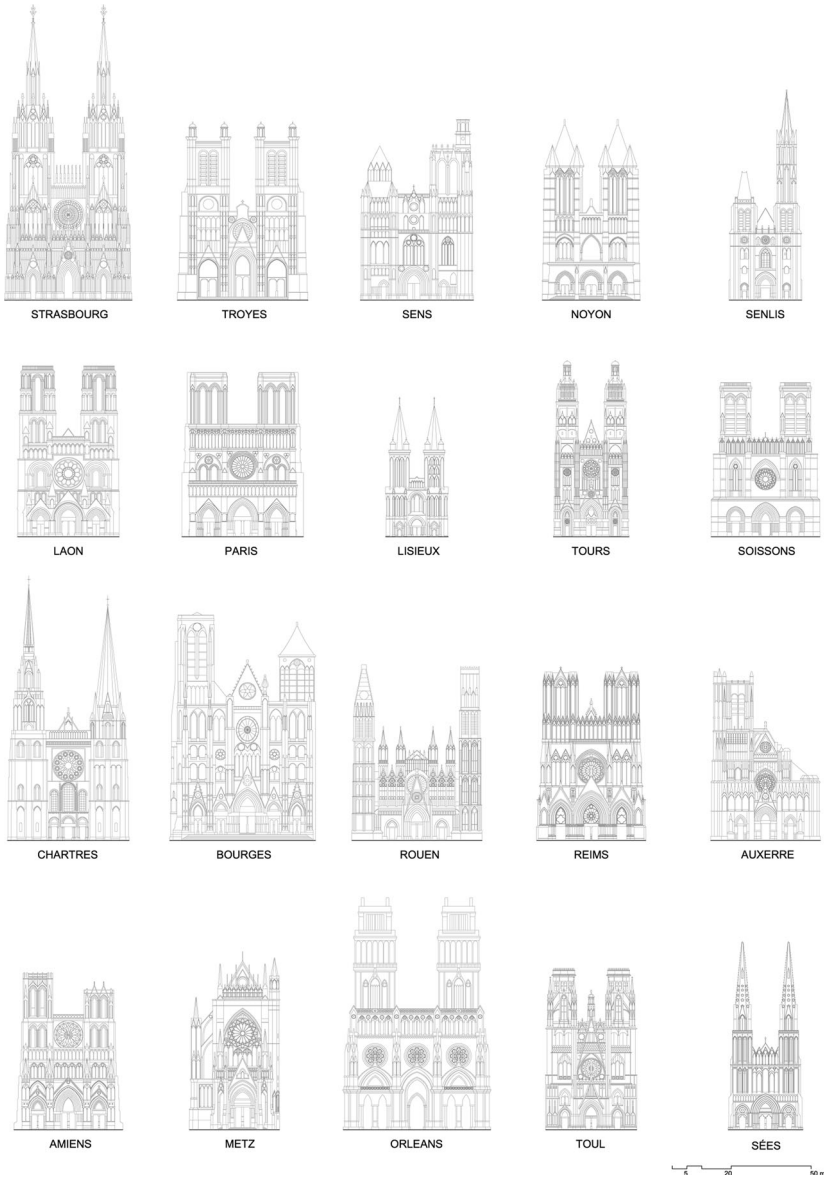

Fig. 8 Main elevations of the cathedrals being studied, in chronological order

a homothetic object, then $S(M) = H(M)$. If M is a self-similar object and $S(M) \neq T(M)$, then M is a fractal object.

In Falconer (1990) and also in other books, the reader can find that:

1. $T(M) \leq \mathcal{H}(M) \leq \bar{F}(M) \leq n$
2. If M is a self-similar object, then $\mathcal{H}(M) = F(M) < S(M)$.

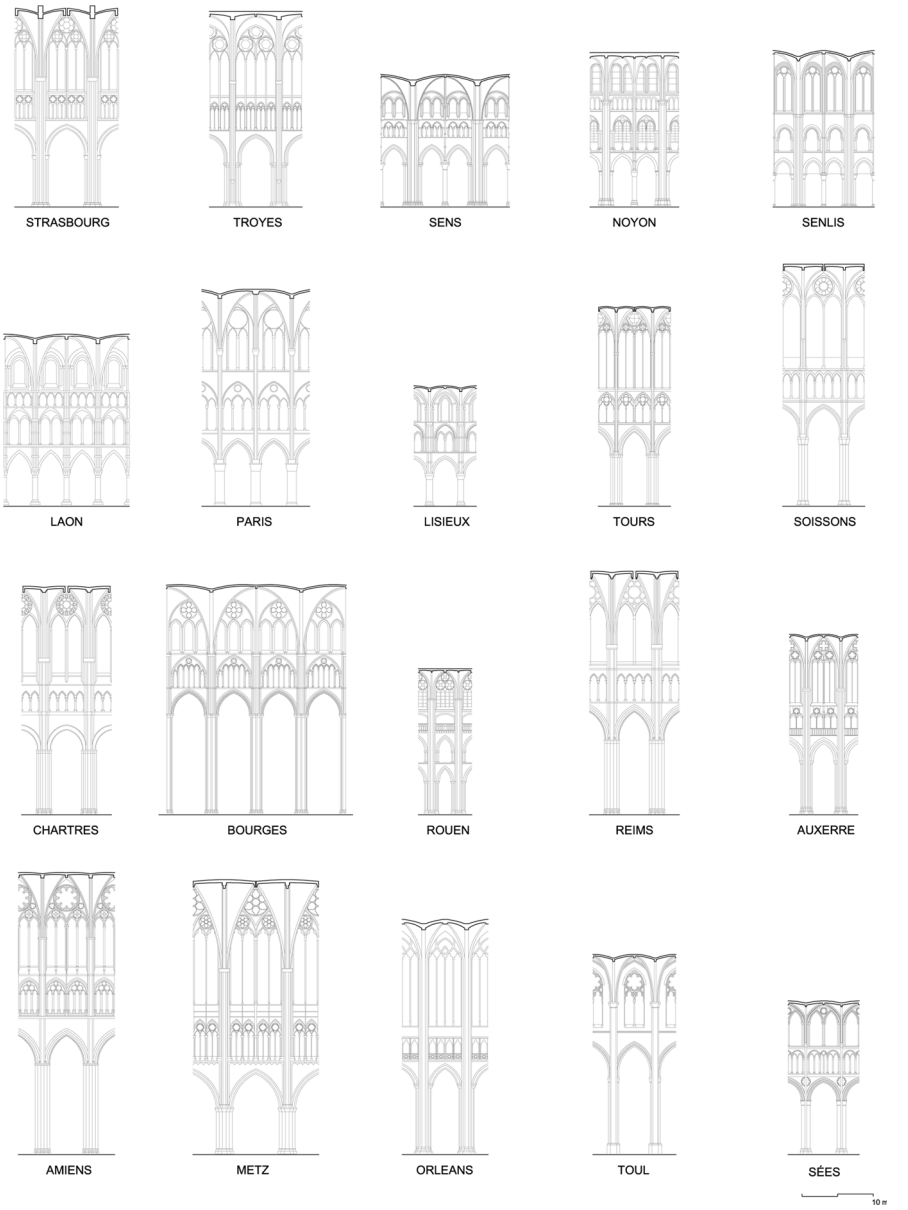

Fig. 9 Cross-sections of the cathedrals being studied, in chronological order

3. If $M = \coprod_{i=1}^{i-m} S_i(M)$ is a self-similar object and there exists a non-empty bounded open set $V \subset \mathbb{A}^n$ such that $V \supset \coprod_{i=1}^{i-m} S_i(V)$, then $\mathcal{H}(M) = F(M) = S(M)$.

Fractal Parameter and Calculation Method

After the theoretical base of the upper fractal dimension $\bar{F}(M)$ and the properties mentioned in the former subsection, now we will explain how to generate the fractal parameter $P_s(M)$.

Architectural structures M are not fractal, however we can consider their unevenness, which determines their space-filling ability (i.e. their level of roughness), and we can generate a parameter for those non-fractal objects. This parameter, which we will call *fractal parameter* $P_s(M)$, provides a measure of M's roughness.

Let us see now the step-for-step method to generate the fractal parameter $P_s(M)$, which was summarized in the first subsection. For illustration, Fig. 5 shows the rose window in the transept elevation of Reims cathedral.

Given the architectural structure M, first we generate its design in AutoCad vector format using black color and line width $\sim$0.00 mm, with homogeneous graphic display criteria. From this AutoCad format we obtain the pdf vector format. Figure 4 shows the detail level of the structure.

From the pdf vector format, by means of an image processing software, we generate a black-and-white digital bitmap file N, sized 1,024 $\times$ υ pixels (standard

Table 2 Vectors obtained from the calculations

(s_5, s_6, s_7, s_8)	Plan	Elevation	Section
Strasbourg	(955, 2957, 8256, 23092)	(1532, 5414, 17073, 44325)	(1323, 4386, 12034, 29699)
Troyes	(1530, 4555, 13043, 35786)	(1054, 3465, 10033, 26254)	(1374, 4405, 11715, 28619)
Sens	(1476, 4398, 12486, 35766)	(1166, 3634, 9919, 24561)	(758, 2524, 7675, 21131)
Noyon	(1116, 3430, 9792, 26615)	(1315, 3953, 11315, 29582)	(1391, 4261, 12076, 28501)
Senlis	(1535, 4673, 13513, 37928)	(1500, 4534, 11833, 28228)	(1159, 3760, 11092, 27027)
Laon	(1121, 3726, 10948, 30914)	(1384, 4716, 13904, 35030)	(1033, 3253, 8551, 18751)
Paris	(2083, 6427, 17992, 50208)	(1151, 3805, 12038, 32454)	(1241, 3673, 9682, 23367)
Lisieux	(1217, 3458, 9095, 23534)	(1310, 3844, 10530, 24592)	(1214, 3524, 8307, 18041)
Tours	(1394, 4280, 11882, 31996)	(1848, 6237, 18417, 49724)	(1684, 5272, 14664, 38914)
Soissons	(1144, 3312, 8795, 23510)	(1094, 3613, 10772, 27100)	(1489, 4172, 10338, 23298)
Chartres	(1128, 3654, 10658, 28952)	(1237, 391, 10939, 28075)	(1571, 4888, 12944, 30644)
Bourges	(1084, 3410, 9666, 26764)	(1256, 4165, 11905, 29997)	(1097, 3544, 11158, 31973)
Rouen	(1335, 4044, 10705, 28928)	(964, 3324, 10391, 26682)	(2126, 6453, 17031, 42164)
Reims	(1720, 5023, 14585, 41123)	(1374, 4592, 14584, 40203)	(1579, 4911, 13876, 37304)
Auxerre	(1551, 4582, 12858, 37109)	(1080, 3508, 10260, 25428)	(1746, 5736, 15140, 37738)
Amiens	(1449, 4292, 11624, 30418)	(1128, 3866, 11656, 29874)	(1788, 6127, 18364, 50930)
Metz	(1493, 4509, 11640, 30187)	(1520, 4752, 13326, 33006)	(1405, 4767, 13897, 37464)
Orléans	(1561, 4891, 13181, 35273)	(1199, 3868, 11726, 29260)	(1778, 5168, 12624, 30641)
Toul	(1075, 3065, 8553, 23887)	(1524, 5256, 15170, 39088)	(1211, 3510, 9973, 25873)
Sées	(1162, 3544, 9875, 26931)	(1575, 5060, 15021, 41740)	(1256, 3837, 10523, 25676)

resolution 1,024 horizontal, υ vertical). The size of the image in N is adjusted to full width and height.

We have developed our own software in order to have total control of the calculation and guarantee correctness. Besides, as we said in the first subsection, using this self-created software we generate the fractal parameter $P_s(M)$ based on the definition of the upper fractal dimension $\bar{F}(M)$. The process used is not the slope of a regression line, but the slope of the last point of a continuous graph ln–ln, as we shall now see.

Since N is a pixelated digital image file, the calculation process to generate $P_s(M)$ will have a finite number of steps. The finest mesh used to generate $P_s(M)$ is a 4×4 pixel square mesh, because $4 = 2^n$ gives the finest mesh which is similar to the theoretical meshes of the theorem mentioned in the previous subsection for the theoretical calculation of $\bar{F}(M)$. This is true because the 4×4 pixel squares have inside points and border points. Therefore, in order to calculate $P_s(M)$ we will use four meshes the squares of which are 4, 8, 16 and 32 pixels in length, respectively. The reason to use four meshes is that, as we will see later, $P_s(M)$ is generated with the slope of a function of a continuous graph ln–ln. Using the classical interpolation methods, four points of a function are enough to find a good approximation of that slope. And we should not use more than four interpolation points because of the well-known Runge Phenomenon in numerical calculation.

Table 3 Parameters P_s obtained from the calculations

P_s	Plan	Elevation	Section
Strasbourg	1.54	1.20	1.27
Troyes	1.42	1.33	1.28
Sens	1.55	1.25	1.39
Noyon	1.42	1.30	1.06
Senlis	1.48	1.22	1.10
Laon	1.51	1.21	1.00
Paris	1.52	1.26	1.22
Lisieux	1.39	1.06	1.12
Tours	1.44	1.39	1.41
Soissons	1.47	1.18	1.12
Chartres	1.41	1.32	1.19
Bourges	1.49	1.25	1.42
Rouen	1.52	1.17	1.30
Reims	1.46	1.32	1.41
Auxerre	1.59	1.16	1.35
Amiens	1.39	1.22	1.44
Metz	1.46	1.21	1.41
Orléans	1.48	1.12	1.36
Toul	1.49	1.31	1.28
Sées	1.47	1.43	1.20

Then (see Fig. 5), our software generates a square mesh, which we have called g_5, consisting of $32 \times h_5$ square boxes with an edge dimension $a_5 = 1,024 \times 2^{-5} = 32$pixels. Then we apply that mesh on the image of N and we calculate $ln(s_5)$, where s_5 is the number of boxes of g_5 which have black pixels. Then we repeat the process with the other square meshes g_6, g_7 and g_8 having $64 \times h_6$, $128 \times h_7$, $256 \times h_8$ square boxes, respectively. The edge dimensions are $a_6 = 1,024 \times 2^{-6} = 16, a_7 = 1,024 \times 2^{-7} = 8$ and $a_8 = 1,024 \times 2^{-8} = 4$, respectively (see Fig. 5). Then we calculate $ln(s_6), ln(s_7)$ and $ln(s_8)$, where s_6, s_7 and s_8 are the number of boxes with black pixels in each mesh g_6, g_7 and g_8, respectively. For example, Table 1 shows the data corresponding to Fig. 5: (h_5, h_6, h_7, h_8 = (32, 64, 128, 256), (s_5, s_6, s_7, s_8) = (799, 2689, 8236, 22294).

As a result of the above mentioned process we obtain the coordinates of four points $(\ln(2^5), \ln(s_5)), (\ln(2^6), \ln(s_6)), (\ln(2^7), (\ln(s_7)), (\ln(2^8), \ln(s_8))$ in a graph ln–ln.

Figure 6 shows the four points which result from Table 1. Now, our software calculates the slope of the continuous graph ln–ln on the fourth point [$\ln(2^8)$, $\ln(s_8)$]. Such slope is an extrapolation of the process used to calculate the theoretical limit of the upper fractal dimension $\bar{F}(M)$. To confirm that the preceding claim is true, you can consider $ln(2^n) = x, ln(s_n) = f(x), \frac{ln(s_n)}{ln(2^n)} = \frac{f(x)}{x}$ and use l'Hôpital's rule. In order to calculate that slope, the software implements the classical four-point formula

Table 4 Parameters P_r obtained from the calculations

P_r	Plan	Elevation	Section
Strasbourg	1.53	1.62	1.49
Troyes	1.52	1.54	1.46
Sens	1.53	1.46	1.60
Noyon	1.52	1.50	1.46
Senlis	1.54	1.41	1.52
Laon	1.59	1.55	1.39
Paris	1.53	1.61	1.41
Lisieux	1.42	1.41	1.29
Tours	1.50	1.58	1.51
Soissons	1.45	1.55	1.32
Chartres	1.56	1.50	1.43
Bourges	1.54	1.52	1.63
Rouen	1.47	1.60	1.43
Reims	1.53	1.63	1.52
Auxerre	1.52	1.52	1.47
Amiens	1.46	1.58	1.61
Metz	1.44	1.48	1.58
Orléans	1.49	1.54	1.36
Toul	1.49	1.56	1.48
Sées	1.51	1.58	1.45

$y_3' \simeq \frac{1}{6h}(-2y_0 + 9y_1 - 18y_2 + 11y_3)$, where $h = \ln 2$ and $y_i = ln(s_{5+i})$. The final result y_3' given by our software is the fractal parameter $P_s(M)$. In the example used in Fig. 5, the fractal parameter is $\frac{1}{6\ln 2}(-2\ln(799) + 9\ln(2689) - 18\ln(8236) + 11\ln(22294)) \simeq 1.33$.

Variants of the Fractal Parameter

We have explained that the fractal parameter $P_s(M)$ is generated by means of the slope in the fourth point of the continuous graph ln–ln. However, in the theoretical cases of fractal self-similar objects such a graph is a straight line. Therefore, if we generate a fractal parameter under the hypothesis of self-similarity, then we can use the slope of the regression line corresponding to the discrete set of the four points belonging the graph $ln - ln$. So, the calculation is the quotient of the covariances $\frac{\sigma_{xy}}{\sigma xx}$ where $\sigma_{xy} = \frac{1}{4}\sum_{i=0}^{i=4}(y_i - \bar{y})((5+i)\ln 2 - \bar{x}), \sigma xx = \frac{1}{4}\sum_{i=0}^{i=4}((5+i)\ln 2 - \bar{x})^2, \bar{x} = \frac{5+6+7+8}{4}\ln 2, \bar{y} = \frac{y_0+y_1+y_2y_3}{4}$. This fractal parameter will be called $P_r(M)$. In the case of the rose window displayed in Fig. 5, we have $P_r(M) \simeq 1.60$.

Some commercial software like Benoit 1.31, by TruSoft Int'l Inc, allow generation of $P_r(M)$ from the pixel file N. In this situation, of course, the value $P_r(M)$ obtained with our software is the same as the value obtained with Benoit.

When many calculation steps are used, with more meshes, commercial software always uses the slope of the regression line. For instance, Benoit 1.31 uses 22

Table 5 Parameters P_b obtained from the calculations

P_b	Plan	Elevation	Section
Strasbourg	1.60624	1.57518	1.49741
Troyes	1.60898	1.51084	1.44870
Sens	1.61128	1.48047	1.52771
Noyon	1.59964	1.49272	1.74688
Senlis	1.62527	1.44926	1.48583
Laon	1.63119	1.52501	1.41866
Paris	1.63493	1.56197	1.40060
Lisieux	1.53833	1.41831	1.36375
Tours	1.59779	1.56567	1.49519
Soissons	1.55476	1.46949	1.34814
Chartres	1.59455	1.48041	1.45659
Bourges	1.62432	1.52556	1.56154
Rouen	1.57932	1.55053	1.51279
Reims	1.61244	1.59039	1.50352
Auxerre	1.61642	1.49271	1.47486
Amiens	1.56189	1.54350	1.56477
Metz	1.54586	1.49182	1.51680
Orléans	1.58828	1.50319	1.42449
Toul	1.58842	1.54721	1.44217
Sées	1.59304	1.53743	1.44756

meshes as default variables: the edge of the widest square mesh is 256 pixels long; each of the following meshes has an edge length equal to the preceding edge length divided by 1.3. The new parameter thus generated will be called $P_b(M)$. Taking the example of Fig. 5, we have $P_b(M) \simeq 1.41$.

As we have commented in "Summary of the Fractal Parameter's Generation Process", if M is not a fractal object nor a self-similar object, then the parameter $P_s(M)$ is more approximated to the theoretical calculation of $\bar{F}(M)$ than $P_r(M)$ and $P_b(M)$. Therefore $P_s(M)$ is lower than $P_r(M)$ and $P_b(M)$ because $\bar{F}(M)$ goes to the minimum value 1.

Redrawing and Calculation

Figures 7, 8 and 9 show the floor plans, main elevations and central cross-sections of the 20 cathedrals being studied. Table 2 shows the vectors (s_5, s_6, s_7, s_8) obtained from the calculations:

According to the values listed in Table 2, we calculate the fractal parameters P_s and P_r for the 20 cathedrals and their three basic projections. Tables 3 and 4 show these parameters.

Table 5 shows the results for the fractal parameter P_b with the five decimal digits given by the commercial software:

Table 6 Means obtained from the calculations

m_i	P_s	P_r	P_b
Strasbourg	1.33	1.55	1.56
Troyes	1.34	1.51	1.52
Sens	1.40	1.53	1.54
Noyon	1.26	1.49	1.61
Senlis	1.27	1.49	1.52
Laon	1.24	1.51	1.52
Paris	1.33	1.52	1.53
Lisieux	1.19	1.38	1.44
Tours	1.41	1.53	1.55
Soissons	1.25	1.44	1.46
Chartres	1.30	1.49	1.51
Bourges	1.39	1.56	1.57
Rouen	1.33	1.50	1.55
Reims	1.40	1.56	1.57
Auxerre	1.37	1.51	1.53
Amiens	1.35	1.55	1.56
Metz	1.36	1.50	1.52
Orléans	1.32	1.47	1.51
Toul	1.36	1.51	1.53
Sées	1.37	1.51	1.53

Results and Discussion

Fractal geometry has often been used to study certain elements of architecture, but this is the first time that it has been used to find a new geometric pattern in the French Gothic architecture.

After studying the 20 most important French Gothic cathedrals, in the preceding section of this paper, we have found the means of their respective floor plans, main elevations and center cross-sections. Table 6 shows the means m_{si}, m_{ri} *and* m_{bi}, expressed with two decimal digits, for the fractal parameters P_s, P_r *and* P_b, respectively.

We will show that the fractal parameters P_r and P_b in Table 6 have a very strong linear correlation among them, so we can consider the fractal parameters P_s and P_r only. From Table 6 we can see that the total mean m_r of the data from P_r is $m_r \simeq 1.50$ and the total mean m_b of the data from P_b is $m_b \simeq 1.53$. The standard deviation of the 20 results from Table 6 is $\sigma_r \simeq 0.041$ for P_r, and $\sigma_b \simeq 0.037$ for P_b. The covariance between the results for P_r and the results for P_b is $\sigma_{rb} \simeq 0.0012$. Therefore, the Pearson correlation coefficient between the two sets of results is $R_{rb} = \frac{\sigma_{rb}}{\sigma_r \sigma_b} \simeq 0.80$, and the Pearson determination coefficient between the two sets of results is $R_{rb}^2 \simeq 0.63$. Using Student's t test with 20–2 degrees of freedom and eight decimal digits (we use eight decimal digits because we want to show the real magnitude of the probability) we reject the null hypothesis of "no correlation between the two sets of results" with a probability $P_{rb} \simeq 0.99998620$. Therefore, in order to study the fractal pattern we will only use the data sets P_r and P_s in Table 6.

Now we will prove that the 20 means m_{si} from Table 6, corresponding to P_s, are very concentrated around their total mean $m_s \simeq 1.33$. To that effect, we calculate the standard deviation of these 20 results, which is $\sigma_s \simeq 0.058$, and the variance $\sigma_s^2 0.0034$. Therefore, Pearson's coefficient of variation $\frac{\sigma}{m}$ is 4 %. In general, when the Pearson coefficient of variation is under 25 % it is considered that there is little scattering around the mean. Since the coefficient in this case is 4 %, we conclude that the total mean m_s is highly representative and shows very little scattering.

Next, we claim that the total mean m_s is a non-random result. To test this claim we will use the well-known Pearson's Chi squared test, and we use eight decimal digits because we want to show the real magnitude of the probability of being a non-random result. We apply Pearson's Chi squared test with 19 degrees of freedom in the following two-way table (Table 7): $I_1 = [1.01, 1.05], I_2 = [1.06, 1.10], \ldots, I_{19} = [1.91, 1.95], I_{20} = [1.96, 2], f_{1,k} = 0, f_{2,k} = 20$ are the obtained frequencies, with the following exceptions: $f_{1,4} = f_{1,9} = 1$, $f_{1,5} = 2$, $f_{1,6} = 3$, $f_{1,7} = 6$, $f_{1,8} = 7$,

Table 7 Two-way table of m_s

	I_1	I_2	I_3	I_4	I_5	I_6	I_7	I_8	I_9	I_{10}	...	I_{20}	Total
$m_{si} \in I_k$	0	0	0	1	2	3	6	7	1	0	...	0	20
$m_{si} \notin I_k$	20	20	20	19	18	17	14	13	19	20	...	20	380
Total	20	20	20	20	20	20	20	20	20	20	...	20	400

Table 8 Two-way table of m_r

	I_1	...	I_7	I_8	I_9	I_{10}	I_{11}	I_{12}	I_{13}	...	I_{20}	Total
$m_{ri} \in I_k$	0	...	0	1	1	6	10	2	0	...	0	20
$m_{ri} \notin I_k$	20	...	20	19	19	14	10	18	20	...	20	380
Total	20	...	20	20	20	20	20	20	20	...	20	400

$f_{2,4} = f_{2,9} = 19$, $f_{2,5} = 18$, $f_{2,6} = 17$, $f_{2,7} = 14$, $f_{2,8} = 13$; and $F_{1,k} = \frac{400}{400}$, $F_{2,k} = \frac{7,600}{400}$ are the expected frequencies. Consequently, applying Pearson's Chi squared test with 19 degrees of freedom we conclude that Table 7 is a non-random table, because the probability of being non-random is $P \simeq 0.99999999$.

Now we repeat the study with the 20 means m_{ri} from Table 6.

We will prove that the means m_{ri} from Table 6 corresponding to P_r are very concentrated around their total mean $m_r \simeq 1.50$. To that effect, we calculate the typical deviation of these 20 results, which is $\sigma_r = 0.041$, and the variance $\sigma^2 \simeq 0.0017$. Therefore Pearson's coefficient of variation $\frac{\sigma}{m}$ is 3 %. According to this, we conclude that the total mean is highly representative and shows very little scattering.

Next, we claim that the total mean m_r is a non-random result. To test this claim we will use again the well-known Pearson's Chi squared test, and we use eight decimal digits because we want to show the real magnitude of the probability of being a non-random result. We apply Pearson's Chi squared test with 19 degrees of freedom in the following two-way table (Table 8): $I_1 = [1.01, 1.05], I_2 = [1.06, 1.10], \ldots, I_{19} = [1.91, 1.95], I_{20} = [1.96, 2], f_{1,k} = 0, f_{2,k} = 20$ are the obtained frequencies, with the following exceptions: $f_{1,8} = f_{1,9} = 1, f_{1,10} = 6, f_{1,11} = 10, f_{1,12} = 2, f_{2,8} = f_{2,9} = 19, f_{2,10} = 14, f_{2,11} = 10, f_{2,12} = 18$; and $F_{1,k} = \frac{400}{400}, F_{2,k} = \frac{7,600}{400}$ are the expected frequencies.

Consequently, applying Pearson's Chi squared test with 19 degrees of freedom we conclude that Table 8 is a non-random table, because the probability of being non-random is $P \simeq 0.99999999$.

So, all things considered, the fractal parameters given by the means m_{ri}, m_{si} and m_{bi} have been obtained using a mathematical mechanism and objective results. In addition, these means are highly concentrated around their total means, m_s, m_r and m_b, respectively; and the probability of them being random results is negligible.

Therefore, we claim that the existence of a fractal pattern (which can be measured by any of the three means m_s, m_r or m_b) is a general, non-random property of the French Gothic cathedrals.

Conclusion

The classic patterns of the Euclidean Geometry were used in the construction of the Gothic cathedrals to provide them with proportion and beauty. Still, as well as the Euclidean elements, there is another complex concept in them: the unevenness of

their structures, which determines their space-filling ability, i.e. their level of roughness. The best tool to describe this concept is given by Fractal Geometry, by means of a ratio called fractal dimension. In this paper we use this concept to generate *fractal parameters* which give a measure of roughness. These parameters are not only attributable to Euclidean elements, but also given by the final architectural result of the constructions.

The 20 cathedrals being studied in this paper are a highly representative sample of the French Gothic style, one which prevents arbitrariness. By means of this sample, we analyze the geometry of the resulting construction using new parameters which were unknown until now. Since each construction had its very own authorship and circumstances, we have not gone on to compare cathedrals with each other. Instead, we have examined if the design traits and structures of these constructions have a deeper geometrical sense than was known to us yet.

In this paper we prove that the French Gothic cathedrals do not only follow the Euclidean geometric patterns, but also have another characteristic pattern which is determined by fractal parameters.

We conclude the existence of a general non-random pattern within the fractal dimension of the French Gothic cathedrals.

References

Baldellou, M. 1995. *Catedrales De Europa*. Madrid: Espasa Calpe. (in Spanish).

Batty, M., and P. Longley. 2001. The fractal city. In *AD, Urban Environments*, ed. E.G. Mapelli. New York: Wiley.

Bechhoefer, W., and C. Bovill. 1994. Fractal analysis of traditional housing in Amasya, Turkey. *Traditional Dwellings and Settlements Working Paper Series* 61:1–21.

Bechmann, R. 1985. *Villard de Honnecourt. La Pensée Technique au XI-Iie Siècle et sa Communication*. Paris: Picard Éditeur. (in French).

Bovill, C. 1996. *Fractal geometry in architecture and design*. Boston: Birkhäuser.

Bovill, C. 2008. The doric order as a fractal. *Nexus Network Journal* 10:283–290.

Brown, C.T., and W.R.T. Witschey. 2003. The fractal geometry of ancient Maya settlement. *Journal of Archaeological Science* 30:1619–1632.

Burkle-Elizondo, G. 2001. Fractal geometry in Mesoamerica. Symmetry. *Culture and Science* 12:201–214.

Cooper, J. 2003. Fractal assessment of street-level skylines: a possible means of assessing and comparing character. *Urban Morphology* 7:73–82.

Crompton, A. 2002. Fractals and picturesque composition. *Environment Planning B* 29:451–459.

Edgar, G. 1998. *Integral, probability, and fractal measures*. New York: Springer.

Eglash, R. 1999. *African fractals: modern computing and indigenous design*. New Brunswick: Rutgers University Press.

Falconer, K.J. 1990. *Fractal geometry, mathematical foundations and applications*. Chichester: Willey.

Falconer, K.J. 1997. *Techniques in fractal geometry*. Chichester: Willey.

Hammer, J. 2006. From fractal geometry to fractured architecture: the Federation Square of Melbourne. *Mathematical Intelligencer* 28:44–48.

Joye, Y. 2007. Fractal architecture could be good for you. *Nexus Network Journal* 9:311–320.

Kunst, H., and W. Schekluhn. 1996. *La Catedral de Reims*. Madrid: Siglo Veintiuno. (in Spanish).

Murray, S. 1996. *Notre-Dame, Cathedral of Amiens, the power of change in Gothic*. Cambridge: University of Cambridge.

Ostwald, M.J. 2001. Fractal architecture: late 20th century connections between architecture and fractal geometry. *Nexus Network Journal* 3:73–84.

Ostwald, M.J. 2010. The politics of fractal geometry in Russian paper architecture: the intelligent market and the cube of infinity. *Architecture Theory Review* 15:125–137.
Ostwald, M.J., and J. Vaughan. 2009. *Calculating visual complexity in Peter Eisenman's architecture: a computational fractal analysis of five houses (1968–1976)*. CAADRIA 2009: Proceedings of the Fourteenth Conference on Computer Aided Architectural Design Research in Asia, 75–84.
Ostwald, M.J., and J. Vaughan. 2010. Comparing Eisenman's House VI and Hejduk's House 7: a mathematical analysis of formal complexity in plan and elevation. Aesthetics and design: 21st Biennial Congress of IAEA. Dresden: Technische Universitat.
Ostwald, M.J., and J. Vaughan. 2013. Representing architecture for fractal analysis: a framework for identifying significant lines. *Architectural Science Review* 56(3):242–251.
Ostwald, M.J., Vaughan, J., and S. Chalup. 2008. A computational analysis of fractal dimensions in the architecture of Eileen Gray. Biological processes and computation: Proceedings of the 28th Annual Conference of the Association for Computer Aided Design in Architecture (ACADIA), 256–263.
Prache, A. 2000. *Cathedrals of Europe*. Cornell: University Press.
Rian, I.M., J.H. Park, H.U. Ahn, and D. Chang. 2007. Fractal geometry as the synthesis of Hindu cosmology in Kandariya Mahadev temple, Khajuraho. *Building and Environment* 42: 4093–4107.
Sala, N. 2006. Fractal geometry and architecture: some interesting connections. *WIT Transactions on The Built Environment* 86:163–173.
Schütz, B. 2008. *L'art des Grandes Cathédrales*. Paris: Hazan. (in French).
Simon, O. 1985. *La Catedral gótica*. Madrid: Alianza Editorial. (in Spanish).
Toman, R. 1998. *El Gótico. Arquitectura, Escultura y Pintura*. Paris: Konemann. (in Spanish).
Vaughan, J., and M.J. Ostwald. 2009. A quantitative comparison between the formal complexity of Le Corbusier's Pre-Modern (1905–1912) and Early Modern (1922–1928) architecture. *Design Principles and Practices: An International Journal* 3:359–372.
Vaughan, J., and M.J. Ostwald. 2010. Using fractal analysis to compare the characteristic complexity of nature and architecture: re-examining the evidence. *Architectural Science Review* 53:323–332.
Vaughan, J., and M.J. Ostwald. 2011. The relationship between the fractal dimension of plans and elevations in the architecture of Frank Lloyd Wright: comparing the Prairie Style, Textile Block and Usonian Periods. *Architecture Science ArS* 4:21–44.
Wilson, C. 1990. *The Gothic Cathedral, the architecture of the Great Church*. London: Thames and Hudson.

Albert Samper is an Architect who obtained his Ph.D. in Architecture at the University Rovira i Virgili of Tarragona in 2013. Presently, he is an associate professor of Architecture at the same university and his main fields of interest are: Fractal Geometry and the application of Geometry to Architecture.

Blas Herrera is Geometer who obtained his D.Sc. in Mathematics at the University Autònoma of Barcelona in 1994. Presently, he is a full professor of Applied Mathematics at the University Rovira i Virgili of Tarragona. His main fields of research interest are: Classical and Differential Geometry, and the application of Geometry to Architecture, Fluid Mechanics and Engineering.